

EXPERIMENTAL ASSESSMENT OF A SEISMIC STRENGTHENING SOLUTION FOR STONE MASONRY WALLS USING A WOODEN STRUCTURE

A. Arêde¹, P. Mendes², B. Silva³, J. Guedes¹, J. Faria¹ and A. Costa⁴

¹ *Aux. Professor, Dept. of Civil Engineering, Faculty of Engineering of University of Porto, Porto, Portugal*

² *Research Assistant, Dept. of Civil Engineering, Polytechnic Institute of Viseu, Viseu, Portugal*

³ *MSc, Dept. of Civil Engineering, Faculty of Engineering of University of Porto, Porto, Portugal*

⁴ *Full Professor, Dept. of Civil Engineering, University of Aveiro, Aveiro, Portugal*

ABSTRACT :

This paper aims at assessing the efficiency of a strengthening procedure using wooden grids applied to stone masonry walls, built and tested in laboratory conditions. The walls were first tested under cyclic horizontal loads to simulate the effects of horizontal seismic action. The experimental response allowed evaluating the cyclic behavior and estimating strength, stiffness, energy dissipation and available ductility of the walls in their original conditions. Afterwards, the walls were retrofitted and further strengthened using an envelope wooden grid to provide external confinement and adopting two different schemes for the connections between the wooden bars. Walls were tested again using the same setup, loading and boundary conditions. Test results are briefly presented, discussed and finally compared in order to assess the effectiveness of the applied strengthening solution. Results are quite encouraging as demonstrated by the significant increase of available ductility and amount of dissipated energy.

KEYWORDS: Stone masonry, wood reinforcement, energy dissipation, ductility

1. INTRODUCTION AND OBJECTIVES

It is increasingly accepted that traditional construction types should be kept and further encouraged for worldwide sustainable construction and built heritage preservation. However, seismic events continuously show that traditional constructions, most of them non-engineered ones, are poorly compatible with seismic demands as evidenced during recent earthquakes in Iran, Peru, Turkey, India (Langenbach, 2003), (Langenbach, 2006).

Looking back to existing ancient buildings some solutions can be found concerning masonry wall reinforcement resorting to wood elements (Touliatos, 2005), (Gulkan and Langenbach, 2004) that performed well in resisting earthquakes. However, these solutions typically include wood reinforcement within the masonry core itself, which means that it cannot be easily adopted for strengthening of existing unreinforced walls.

Bearing in mind these two basic issues, the present paper deals with the aim of developing suitable strengthening techniques for traditional stone masonry construction by using, or simply activating, other elements normally present in common buildings. It is the case of wood elements existing in floors or roofs that contribute for the overall behavior provided they are suitably connected to masonry walls. However, other types of architectural elements traditionally made of wood, might be of some use for structural purposes by providing additional strength for wall panels. The key issue is therefore to develop feasible ways of introducing new wood elements in existing masonry walls.

In line with this scope, the paper reports on an experimental campaign on traditional type stone masonry wall panels tested under in-plan horizontal cyclic reversals with constant axial load. Traditional master builders have constructed lime mortared irregular stone masonry panels inside the Laboratory for Earthquake and Structural Engineering (LESE) of the Faculty of Engineering of University of Porto (FEUP).

Wall panels were first tested to assess their original condition behavior up to a damage extent compatible with subsequent repair consisting of stone repositioning, joint repointing and panel reinforcing with an external wood grid enveloping the masonry. For these first trials, the reinforcement was intended for overall confinement of the masonry panel and for shear behavior enhancement. Subsequently, panels were tested again, at least for the same loading history as for the original one, and results of both tests are compared in order to assess the response

improvement in terms of strength, ductility and energy dissipation capacity. Up to now two of such panels were tested in both original and strengthened conditions, but adopting different strengthening solutions and the results are quite encouraging as evidenced in the following sections.

2. SPECIMENS AND EXPERIMENTAL SETUP

2.1. Non-Reinforced Walls PA1_NR and PA2_NR

The experimental study was based on two irregular stone masonry wall panels (PA1 and PA2) built at the LESE - of FEUP. Figure 1 includes views of some construction stages of one of the walls.

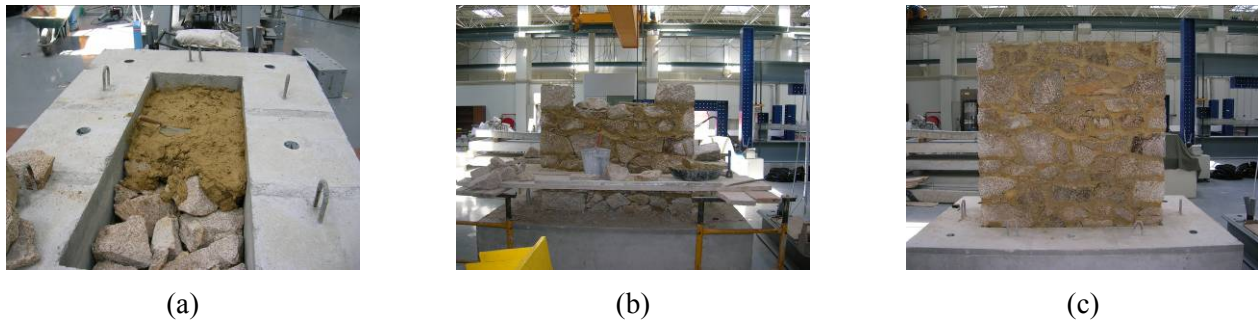


Figure 1 Construction stages of stone masonry walls

The tested specimens consisted of two-leaf irregular masonry wall panels, 1.6m long, 1.6m high and 0.6m thick. The wall leaves are made of good quality granite stones placed in layers along both sides of the wall and using lime mortar in between the stones. Some of the stones were positioned along the transverse direction of the walls in order to connect the leaves as commonly found in some types of multiple-leaf walls. The walls were built on a $1.6 \times 2.6 \times 0.6 \text{ m}^3$ reinforced concrete base in order to simulate a rigid foundation as shown in Figure 2. In their original conditions, i.e. before testing, walls were designated as PA1_NR and PA2_NR.

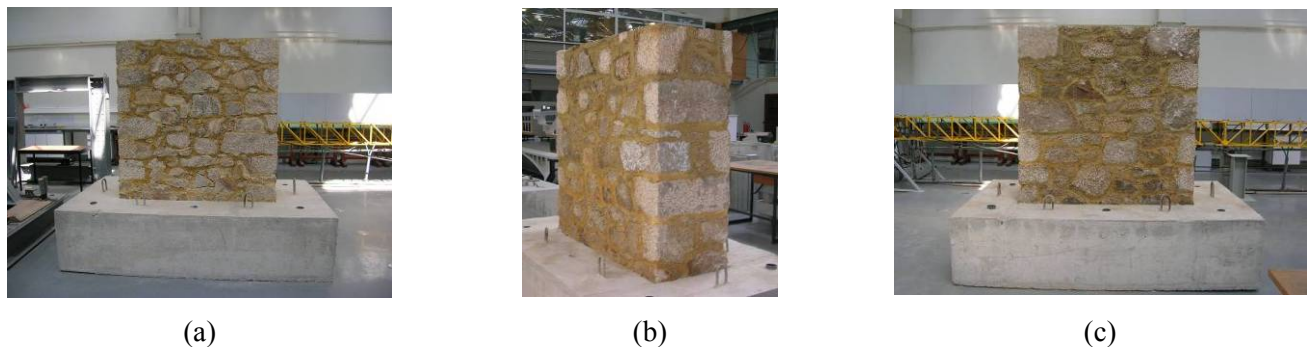


Figure 2 Tested walls. (a) PA1 – lateral view. (b) PA1 – side view. (c) PA2 – lateral view.

Walls were tested under constant vertical force and in-plane horizontal cyclic controlled displacements. This experimental campaign allowed assessing the walls' behavior and its main characteristics, such as energy dissipation, stiffness and strength.

2.2. Reinforced Walls PA1_RM1 and PA2_RM1

After the first tests on each of PA1_NR and PA2_NR walls, the specimens were repaired by placing again the blocks in original positions using new mortar with the same characteristics of the original one. In addition, each panel was strengthened with wood members around the wall according to the configurations shown in Figure 3, mainly aiming at improving the panel confinement. For that reason the new wood bars were not directly fixed to the wall. After strengthening, the walls were designated by PA1_RM1 and PA2_RM1.

For wall PA1_RM1 three horizontal wood bars were adopted on each face and attached to lateral grids, each one made of two vertical and four horizontal bars. All members have cross-section dimensions: 0.04m x 0.06m. Connections of horizontal members of wall faces to lateral grids were made with metal plates (3mm thick) and screws (5mm diameter).

As for wall PA2_RM1, only two horizontal wood bars were used, along with two crossed bars on each face with 0.026m x 0.065m cross section dimensions. These members are also attached to lateral grids as in PA1_RM1 wall, but in this case with just three horizontal bars; all the bars of these grids have 0.020m x 0.065m cross section dimensions. Connections of wall face bars to the grids were made using screws (4 mm diameter).

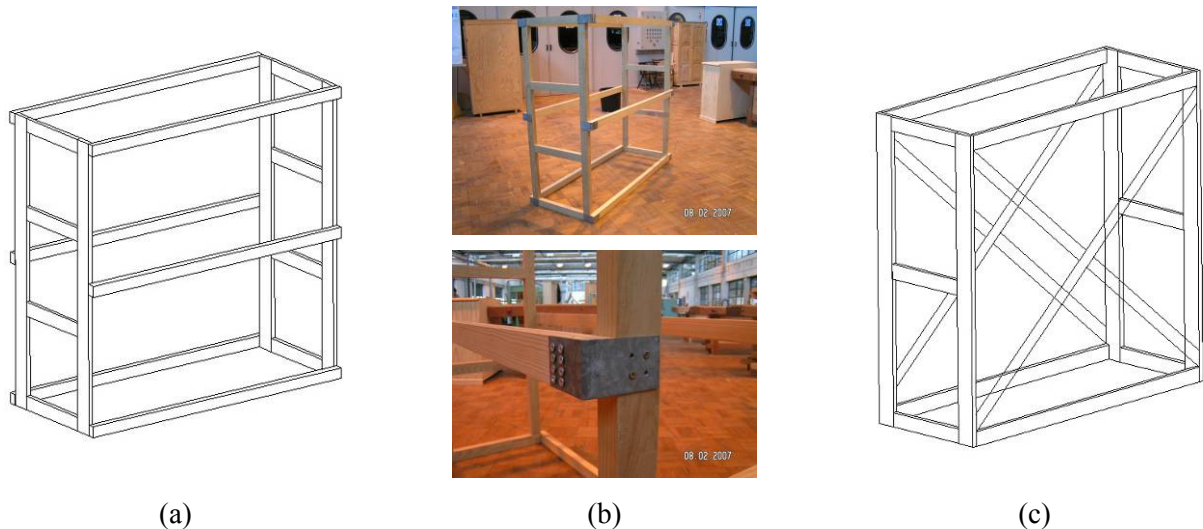


Figure 3 Wood reinforcement. (a) PA1_RM1. (b) Wood members and connection details. (c) PA2_RM1.

2.3. Experimental Setup

The walls were tested under a constant vertical load of 50kN corresponding to a compression level of approximately 52kPa and cycled under controlled in-plane horizontal displacements. The horizontal load was applied at the top of the walls by means of a hydraulic actuator (100kN capacity, +/- 100mm stroke and hinged at extremities) and using a steel reaction frame (Figure 4 (a)). The vertical force was applied to the top section of the walls by means of two other hydraulic jacks (Figure (4a)) and the corresponding total force was measured with load cells. Each pair of jacks was reacting against a steel beam connected to the concrete foundation block by means of two steel rods where load cells were installed. The foundation block was attached to the laboratory reaction floor using four high-strength pre-stressed rods in order to minimize displacements of the block during the test; these rods were monitored by means of glued strain gauges to check possible fluctuations of vertical load. Displacements were measured using classical LVDTs (Linear Variable Displacement Transformers) with different ranges (from +/- 10mm to +/- 100mm) depending on the expected motion of measurement point. Horizontal displacements were measured near the lateral force level and in-height along both wall sides (north and south) to obtain the deformed profile of the wall. In addition, vertical opening/closing motions in horizontal joints of wall sides were measured using short range LVDTs and another pair of transducers was also placed orthogonal to the East wall face to monitor any possible out-of-plane displacement or rotation. Figure 4 (c) provides the general layout scheme of displacement transducers, some of which can be seen in Figure 4 (b); in total, 29 LVDTs were used for PA1_NR wall tests and 26 for the PA2_NR panel.

The horizontal actuator was displacement controlled using a PXI controller system from National Instruments (ni.com) and specifically home developed control routines based on the LabVIEW software platform (also from National Instruments). Similarly, the data acquisition is based on another PXI system equipped with acquisition and signal conditioning cards that allow direct data reading from strain gauges, load cells, LVDTs and other types of amplified analogical or digital sensors. The data acquisition software was identically developed in LabVIEW.

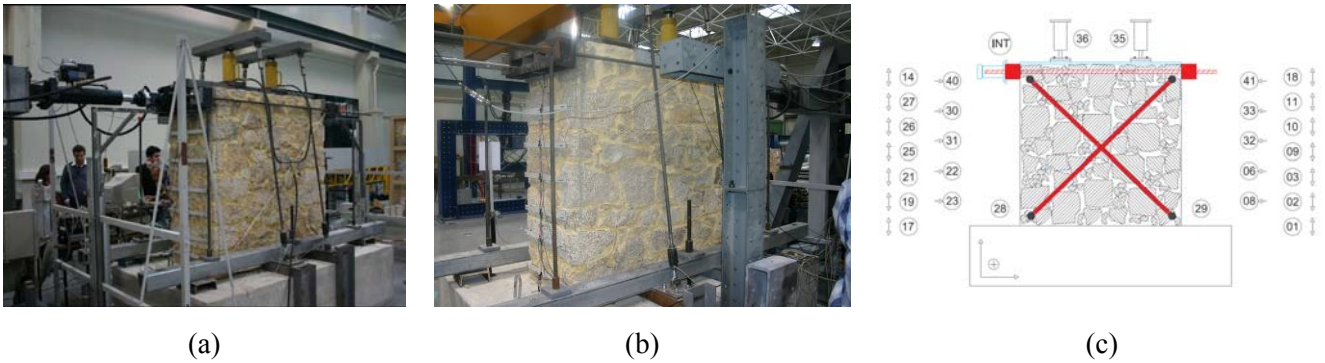
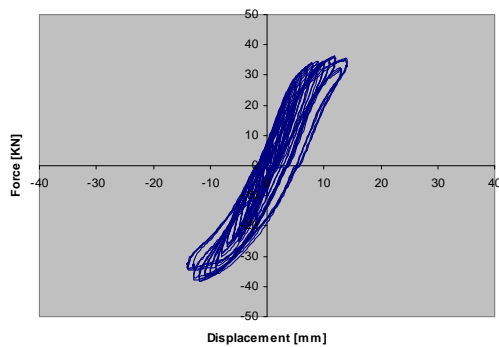


Figure 4 Test setup. (a) North-west view. (b) South-east view. (c) Positions of LVDTs on West face.

3. TESTS AND RESULTS

Tests were quasi-statically performed by imposing a top-displacement time-history of increasing amplitude, with three cycles for each target displacement. For the present study purpose, the main results consist of the top force-displacement diagrams representative of the wall global response. Therefore, results are analyzed in terms of such diagrams and of some calculations made for energy dissipation, ductility and bilinear idealization of the response. Since the study focuses on the comparison of original and strengthened wall panels, the following figures include the obtained force-displacement curves and the final damaged state for each tested specimen. Figures 5 and 6 refer to PA1_NR and PA1_RM1, respectively, whereas Figures 7 and 8 include the results from PA2_NR and PA2_RM1 tests.

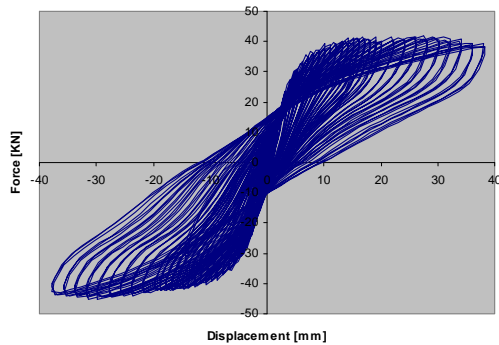


(a)



(b)

Figure 5 PA1_NR. (a) Force-Displacement curve. (b) Final damage in West face.

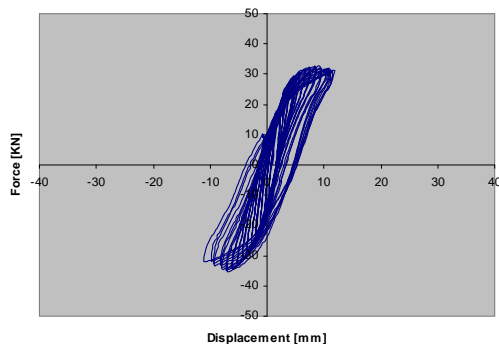


(a)



(b)

Figure 6 PA1_RM1. (a) Force-Displacement curve. (b) Final damage in East face.

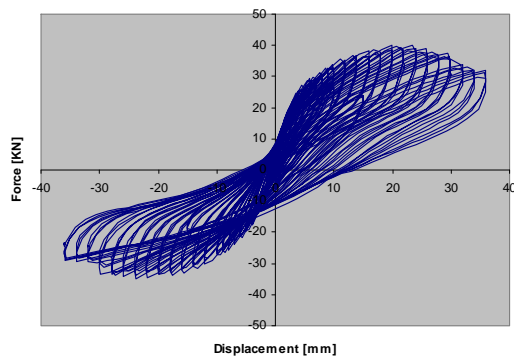


(a)



(b)

Figure 7 PA2_NR. (a) Force-Displacement curve. (b) Final damage in West face.



(a)



(b)

Figure 8 PA2_RM1. (a) Force-Displacement curve. (b) Final damage in East face.

4. DISCUSSION AND RESULTS ANALYSES

Results for the original walls evidenced shear-controlled responses as confirmed by the damage patterns where diagonal cracking/joint opening became quite visible. Due to unavoidable construction differences, wall panel PA1_NR exhibited better response than PA2_NR, not only because a slightly larger strength was reached (for the same vertical load in both walls) but also because the final damage distribution was found less strong. For these first tests, imposed displacements were limited to about 14mm for PA1 and 11mm for PA2, which was not *a priori* defined but became necessary in order keep wall damage within acceptable limits to allow subsequent wall repair and testing under strengthened conditions.

Despite the fact that drifts were not pushed further (maximum imposed about 0.9% for PA1_NR), the response diagrams of the non-reinforced walls clearly show the onset of strength degradation in both loading senses; however, this effect is more evident for negative sense, i.e. towards the north (actuator) side as shown in Figures 5(a) and 7(a). This means that, should larger displacements be imposed, wall strength would have dropped fast and complete failure would have occurred. Detailed analysis of non-strengthened walls is provided by Silva (2008).

Notwithstanding this pre-failure stage, energy dissipation was found significant and developing at a stable rate (and even slightly increasing) as shown in Figure 9 where the evolutions of dissipated energy are plotted for all tested specimens. These plots have been divided in correspondence with positive and negative half-cycles and, therefore, allow evaluating the amount of energy dissipated up to a given value of positive or negative displacement. It is particularly relevant that this type of walls, made of quite irregular stone masonry and poor mortar, exhibits such regular and well proportioned force-displacement loops responsible for interesting energy dissipation, even slightly larger than the strengthened wall for the case PA2 (Figure 9). This evidence is clearly related with internal friction between adjacent stone blocks (and surrounding mortar, as well) that provides an excellent means of energy dissipation as long as the whole wall aggregate keeps working together. In a word, this is the basic idea of the proposed strengthening scheme that seeks for a suitable external confinement effect to prevent masonry from disaggregating.

Although the scheme is not new, because in fact it has been adopted with other materials (like steel meshes or similar), the fact that resort is made to wood is much more unusual (even likely to be of some originality, at least from the knowledge of the authors). Moreover, if these wood members are made thin enough to be compatible with other architectural elements, often existing in this type of old masonry constructions, than the proposed scheme can be very attractive in the framework of seismic rehabilitation of traditional masonry constructions.

Focusing now on the results of tests after strengthening as previously described, the force-displacement diagrams shown in Figures 6(a) and 8(a), for strengthened wall panels PA1_RM1 and PA2_RM1, respectively, clearly show an impressive increase of ductile capacity of that “confined masonry”. Visual inspection of the response curves show that global ductility factors between 7 and 8 can be found, even for the case of PA2_RM1 where more pronounced strength degradation was observed. Again, this is consistent with the evolution of dissipated energy (Figure 9) that shows increasing rate for increasing amplitude of cyclic displacements.

It is noteworthy that panel PA1 exhibited almost the same energy dissipation before and after repair and strengthening during the first cycles with the same displacement levels (PA1_NR and PA1_RM1 curves almost coincide for positive and negative senses in Figure 9). This means that, on the one hand the masonry repair was efficient enough to replace the wall capacity; on the other hand, it shows that the wood strengthening only became effective for larger displacement levels, once the masonry reached sufficient dilation and started to mobilize the wood cage confinement effect. Finally, the symmetry of force-displacement diagram for PA1_RM1 (Figure 6(a)) is also reflected in the almost identical evolution of dissipated energy for both displacement senses (Figure 9), which is consistent with the final damage observed in the wall.

Concerning the PA2_RM1 specimen, somewhat opposite conclusions can be drawn. Although the strengthening outcome was clearly advantageous, both in terms of available ductility (Figure 8(a)) and energy dissipation capacity, the performance was not improved for the first displacement cycles when compared with the non-reinforced PA2 wall. In fact, energy dissipation was lower for the PA2_RM1 test than for PA2_NR, particularly for the negative sense; similarly, the strength for PA2_RM1 degrades much more than PA1_RM1 and, again for the negative sense, it dissipates energy less efficiently. This agrees with the fact that PA2 was of worse quality than PA1 (essentially concerning stone block arrangement) and with the observed final damage shown in Figure 8(b) when compared against that in Figure 6(b).

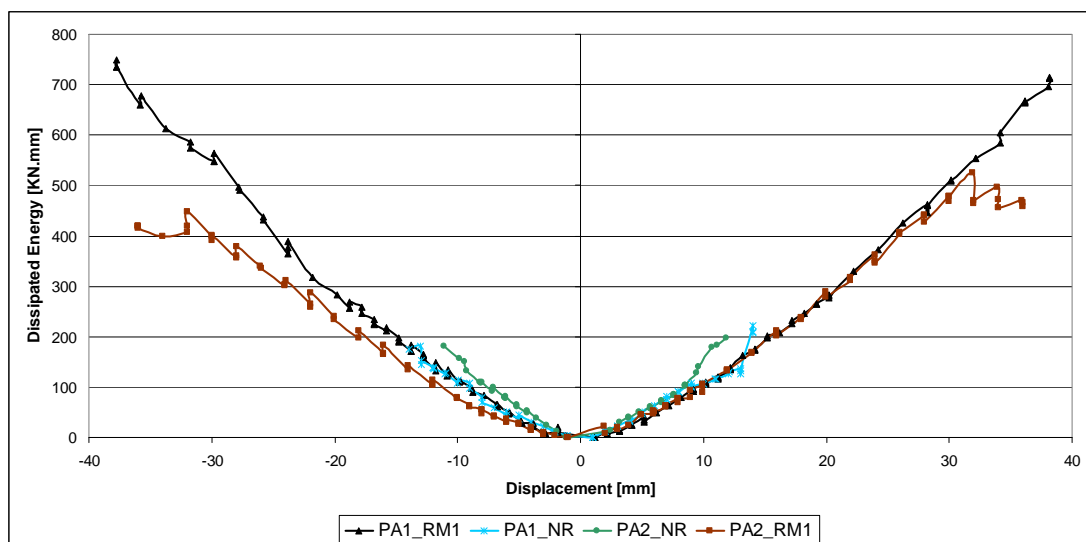


Figure 9 Energy Dissipation

The lower efficiency of the strengthening scheme based on diagonal wood bars as adopted in PA2_RM1, when compared with PA1_RM1, is related with the following reasons: *i*) the lack of longitudinal bars to link the opposite side grids, that have proved to be essential to ensure the masonry integrity, in the middle zone where dilation effects are more pronounced; *ii*) more reduced bar thickness compared with that of PA1_RM1; *iii*) the absence of steel angle plates in the connections of longitudinal bars to side grids that, in the case of PA1_RM1 case, played an important role in dissipating energy, confirmed by the plastic deformations observed in the plates.

Attempting to quantify the behavior improvement due to the wood strengthening process, and resorting to Tomažević proposal (Tomažević, 1999), a bilinear approximation was made to the envelope of the hysteretic force-displacement response curves (assuming the envelope as representative of the monotonic response diagram). As shown in Figure 10, by considering equal energy dissipation both in experimental envelope curve and in the idealized bilinear diagram, it is possible to calculate F_u according with Eqn. 4.1, where A is the area below the experimental curve, corresponding to dissipated energy, K_e is the initial stiffness estimated from that curve upon adequate selection of the cracking point (F_{cr}, d_{cr}) and d_{max} is the maximum displacement reached in the experimental curve.

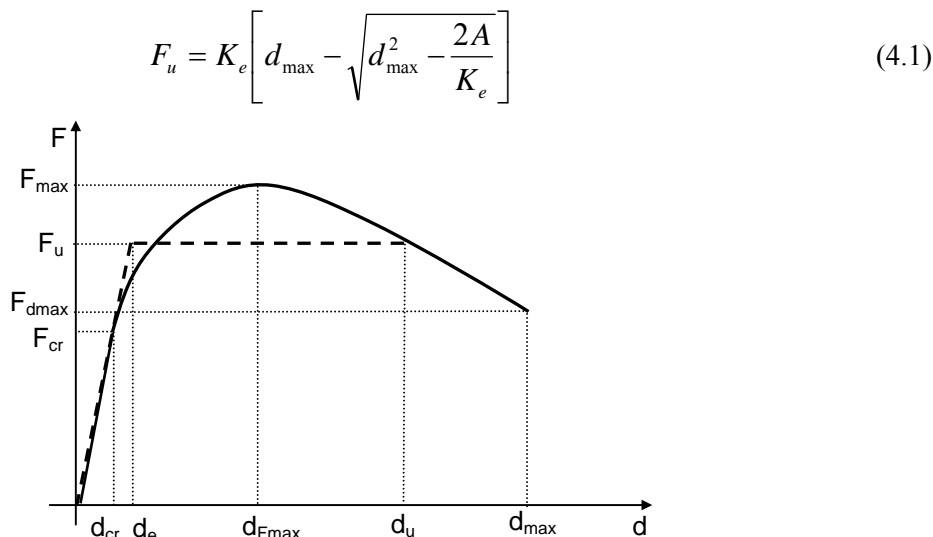


Figure 10 Bilinear approximation to the diagram envelope

The experimental envelope curve was defined by considering the positive force sense and the maximum displacements points of each hysteresis loop. Adopting this procedure for the four tested walls, leads to the results presented in Table 4.1 that allow estimating available ductility defined as the ratio between the ultimate idealized displacement, d_u , and the displacement at the idealized elastic limit, d_e (according to Figure 10).

Table 4.1 Data results for bilinear diagram approach

Wall	F_{cr} (KN)	d_{cr} (mm)	K_e (KN/mm)	F_{max} (KN)	d_{Fmax} (mm)	d_{max} (mm)	F_u (KN)	d_e (mm)	d_u (mm)	μ_u (d_u / d_e)
PA1_NR	19.83	3.04	6.53	36.36	12.08	14.03	32.65	5.00	13.02	2.60
PA1_RM1	23.15	3.20	7.23	41.85	28.19	38.20	39.61	5.48	36.18	6.60
PA2_NR	27.14	3.92	6.92	32.68	9.47	11.84	32.06	4.63	9.62	2.08
PA2_RM1	17.82	1.96	9.08	40.14	23.95	35.97	34.95	3.85	31.94	8.29

As already mentioned before, ductility has a considerable increase from non-reinforced to reinforced walls, due to the above described reasons. Ductility values now obtained agree with the visual estimates above referred. It is worth mentioning that the maximum force, F_{max} , shows some increase from non-reinforced to reinforced walls, but with no relevance taking into account that there was some unexpected variation in axial load (around 10% to 15%) during the test.

5. FINAL REMARKS

Experimental evidence from the tested walls, as reported in the previous sections, show that this type of traditional stone masonry has a good potential for energy dissipation, provided that it is prevented from disaggregating, thanks to the internal friction between adjacent stones and surrounding mortar.

Taking into account the adopted strengthening procedure, reinforced walls have shown a considerably larger lateral deformation capacity in contrast with non-reinforced walls. This was confirmed by quantifying the ductility factor and allows concluding that it can be a good solution to retrofit existing traditional buildings. Indeed, a great improvement of energy dissipation capacity was found in reinforced walls, although with neither significant strength increase nor evidenced changes in stiffness. This means that, as desired, wood reinforcement acts as a selective retrofitting scheme by providing confinement to the wall masonry that prevents from failing.

This study is just a preliminary one, as further tests and analyses are under development. Issues like the influence of pre-compression load variation in the maximum lateral force values are under investigation. New arrangements are being designed, tested and analyzed to look up for feasible, economical and efficient solutions, but results achieved so far show that a quite promising strengthening strategy was found.

ACKNOWLEDGEMENTS

This paper refers research work made with financial contribution of "FCT - Fundação para a Ciência e Tecnologia", Portugal, that is gratefully acknowledged.

REFERENCES

- Gulkan, P. and Langenbach, R. (2004). The Earthquake Resistance of Traditional Timber and Masonry Dwellings in Turkey. *13th World Conference on Earthquake Engineering, Vancouver, Canada*, **Paper n°2297**.
- Langenbach, R. (2003). Survivors amongst the rubble: traditional timber-laced masonry buildings that survived the great 1999 earthquakes in Turkey and the 2001 earthquake in India, while modern buildings fell. *Proceedings of the First International Congress on Construction History, Instituto Juan de Herra, Escuela Técnica Superior de Arquitectura, Madrid*, **Vol. 2, 2003**, 1257-1268.
- Langenbach, R. (2006). Preventing Pancake Collapses: Lessons from Earthquake-Resistant Traditional Construction for Modern Buildings of Reinforced Concrete. *International Disaster Reduction Conference (IRDC), Davos, Switzerland*.
- Silva, B. Q. (2008). Aplicação de um modelo de dano contínuo na modelação de estruturas de alvenaria de pedra – Igreja de Gondar – um caso de estudo. MSc Thesis, FEUP, Porto (in Portuguese)
- Tomažević, M. (1999). Earthquake-Resistant Design of Masonry Buildings, Imperial College Press, London, UK.
- Touliatos, P. (2005). The Box Framed Entity and Function of the Structures. The Importance of Wood's Role. *Proceedings of the International Conference Conservation of Historic Wooden Structures, Florence, Italy*, **52-64**.
- Vintzileou, E. (2008). Effect of Timber Ties on the Behavior of Historic Masonry. *Journal of Structural Engineering ASCE* **June 2008**, 961-972.